Nanoscale

PAPER

View Article Online
View Journal | View Issue

Cite this: *Nanoscale*, 2016, **8**, 6860

Scalable fabrication of high-quality, ultra-thin single crystal diamond membrane windows†

Afaq Habib Piracha,[a] Kumaravelu Ganesan,[a] Desmond W. M. Lau,[a,b] Alastair Stacey,[a] Liam P. McGuinness,[a,c] Snjezana Tomljenovic-Hanic[a] and Steven Prawer*[a]

Received 25th November 2015,
Accepted 1st March 2016

DOI: 10.1039/c5nr08348f

www.rsc.org/nanoscale

High quality, ultra-thin single crystal diamond (SCD) membranes that have a thickness in the sub-micron range are of extreme importance as a materials platform for photonics, quantum sensing, nano/micro electro-mechanical systems (N/MEMS) and other diverse applications. However, the scalable fabrication of such thin SCD membranes is a challenging process. In this paper, we demonstrate a new method which enables high quality, large size (~4 × 4 mm) and low surface roughness, low strain, ultra-thin SCD membranes which can be fabricated without deformations such as breakage, bowing or bending. These membranes are easy to handle making them particularly suitable for fabrication of optical and mechanical devices. We demonstrate arrays of single crystal diamond membrane windows (SCDMW), each up to 1 × 1 mm in dimension and as thin as ~300 nm, supported by a diamond frame as thick as ~150 μm. The fabrication method is robust, reproducible, scalable and cost effective. Microwave plasma chemical vapour deposition is used for *in situ* creation of single nitrogen-vacancy (NV) centers into the thin SCDMW. We have also developed SCD drum head mechanical resonator composed of our fully clamped and freely suspended membranes.

1. Introduction

Diamond is well-known for its exceptional mechanical, thermal and optical properties. Diamond is also a high refractive index and wide band gap material which makes it useful in electronic, thermal and optical applications.[1] Single crystal diamond is unique in that it is known to host more than 500 colour centers ranging from ultraviolet (UV) to infrared (IR).[2] Many colour centers are bright enough to be used as single photon sources and some, most notably the negatively charged nitrogen vacancy (NV^-) centre, display a range of highly desirable quantum properties such as optical single spin read out. Hence, SCD is one of the most promising materials for integrated photonics, optomechanics and quantum information processing (QIP) applications.[3,4]

In exploiting these properties, many applications in the field of photonics and sensing technologies require high quality thin SCD membranes containing bright colour centres.[4] In particular, for optical waveguide and cavity performance, the thickness of the SCD membrane is critical in satisfying the single mode condition in the vertical direction. For applications such as QIP, the thickness of the SCD membrane should be on the order of the ratio between the operational vacuum wavelength and the refractive index of the diamond material.[5] In the case of NV^- centres for which the zero phonon line wavelength is at 637 nm and the refractive index of diamond material is ~2.4, the required thickness should be of the order of ~300 nm. However, macroscopic area, sub-micrometer thick SCD membranes are not commercially available. High quality SCD material with macroscopic sizes can be grown only on diamond substrates, although significant progress is being made with heteroepitaxial growth on silicon *via* iridium/yttria-stabilized zirconia films.[6,7] Broadly speaking, there are three main approaches developed so far for the production of thin SCD membranes.

A conventional process for fabricating thin SCD membranes includes CVD in conjunction with mechanical polishing and chemical etching.[8–16] Recently, SCD plates as thin as ~5–50 μm have become commercially available. However, further polishing and significant RIE thinning is required to achieve the desired sub-micron thicknesses.[8–16] These plates tend to have wedged thickness profiles that result in thickness variations in resultant membranes.[12,13] To date, this has been the most promising approach to fabricate thin SCD membranes and

[a]*School of Physics, University of Melbourne, Victoria 3010, Australia. E-mail: s.prawer@unimelb.edu.au*
[b]*ARC Centre of Excellence for Nanoscale BioPhotonics, School of Science, RMIT University, Melbourne, VIC 3001, Australia*
[c]*Institute for Quantum Optics, University Ulm, Ulm, D-89081, Germany*
†Electronic supplementary information (ESI) available. See DOI: 10.1039/c5nr08348f

employed as a platform for diamond based sensors,[8] radiation detectors,[9] micro/nano-mechanical resonators,[10–12] integrated photonics,[13,14] Raman lasers[15] and frequency combs.[16]

A different method that has been used is the fabrication of 10 μm wide and millimetre long beams with 200 nm thickness by etching 10 μm deep trenches on a bulk SCD using RIE.[17,18] In the last step, thin strips are picked up mechanically from the substrate. But, these membranes have not been used for integrated devices fabrication due to size limitations.

Ion implantation and lift-off is another technique for fabrication of free-standing thin SCD membranes.[19–22] This technique has many advantages. Prime among these is that ion implantation process creates an etchable damage layer at a fixed depth below the surface, and so naturally provides a membrane of uniform thickness that is independent of the parallelism of the original substrate. However, the residual damage from the ion implantation step introduces built-in strain and also degrades the optical quality of the membranes, limiting the use of these membranes for photonic devices.[20] These stand-alone thin membranes also tend to crack and bow during lift-off limiting the production of large size ultra-thin membranes. Nevertheless, CVD overgrowth after ion implantation, can be used to form a high-quality SCD layer followed by plasma etching of the damaged layer and provides a promising platform for photonic device fabrication.[21,22] In order to remove the entire damaged region after CVD overgrowth step, only 1–2 μm of diamond needs to be removed by RIE. Furthermore, a variety of colour centers can be incorporated in the membranes through control of the CVD overgrowth process.[23]

Each of these methods has their own advantages and disadvantages. The disadvantages common to all three methods are the difficulty in handling. To overcome the handling problem, these membranes are often bonded to a substrate such as Si/SiO_2 which may restrict the operational functionality of membranes due to different thermal/chemical properties of the substrate and bonding materials. In addition, scalability is another issue to be addressed. Here we report a robust fabrication method that overcomes many of the SCD processing limitations by providing large, ultra-thin, low-strain SCD membrane windows supported by a thick diamond frame. These membrane window architectures are easy to handle while minimizing breakage/curvature and incorporate single NV centres. The membrane properties are dependent primarily on control of the CVD overgrowth process, which has been shown to produce extremely high quality single crystal material provided sufficient substrate preparation methods are followed to minimize dislocation generation.[24] Furthermore, this fabrication process is suitable for large scale production, by allowing for parallel implantation, overgrowth and etching of multiple membranes.

2. Fabrication

The fabrication process of high quality, ultra-thin SCDMW is shown in Fig. 1. In this work, high pressure high temperature (HPHT) Type 1b and CVD grown Type IIa SCD substrates (300–500 μm thick) were implanted with 1 MeV energy Helium

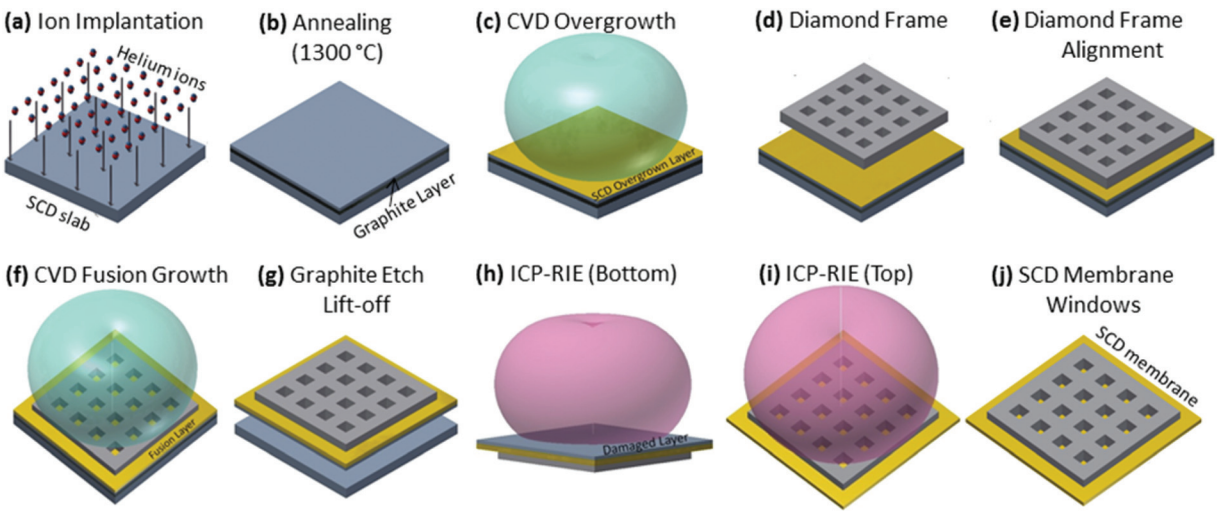

Fig. 1 Schematic of fabrication process of ultra-thin SCD membrane windows (a) The as-received SCD slab was implanted with high energy Helium ions to create a thin damage layer ~1.7 μm deep from the diamond surface. (b) The implanted diamond was annealed at temperature ~1300 °C for 1 hour to convert the amorphous layer to graphite-like etchable carbon layer (c) The annealed diamond was then overgrown using MPCVD yielding high quality SCD layer. (d) Another slab of diamond (PCD or SCD) milled using a laser cutter has lateral dimensions smaller than the original SCD substrate and with a thickness of 150–300 μm. Frames of different geometries such as micro-channels can be fabricated that connect some of the apertures within the diamond frame. (e) The diamond frame was then placed and aligned on the top of the overgrown substrate. (f) The diamond assembly was again grown in MPCVD reactor for selective growth and fusion of diamond frame. (g) The assembly was immersed in an electrochemical cell to etch the graphite-like carbon layer. The SCD membrane fused with the thick diamond frame was lifted off. (h) The fused membrane was flipped and thinned using ICP-RIE to etch the damage layer. (i) If required, RIE was conducted through frame apertures. (j) The finished large area, high quality, ultra-thin SCDMW produced by a scalable process.

ions with a flux of 5×10^{16} ions per cm^2 to create an end-of-range damage layer at ~1.7 μm depth from the diamond surface (Fig. 1a). The end-of-range depth was calculated with Stopping and Range of Ions in Matter (SRIM) simulations.[25] The implanted substrate was then annealed in vacuum (5×10^{-6} mbar) at a temperature of ~1300 °C for 1 hour to convert the end-of-range sub-surface layer to a graphite-like etchable amorphous carbon layer (Fig. 1b).[26,27] The annealed substrate was overgrown using a Cyrannus Iplas microwave plasma chemical vapour deposition (MPCVD) reactor at a growth rate of ~20 nm min^{-1}. The CVD conditions for the high quality homoepitaxial SCD growth were as follows: microwave power 3000 W, pressure 100 Torr, gas mixture composition 2% methane (CH_4) in hydrogen (H_2). The substrate temperature was kept between 950 °C and 1000 °C (Fig. 1c). A total of 10 samples were overgrown to thicknesses ranging between 300 nm and 1 μm for use in different experiments. The diamond frames were fabricated from 150 μm thick diamond slabs (SCD or PCD) using a laser micromachining system (Fig. 1d). Frames of different shapes and geometries can be produced. The diamond frame was then positioned and aligned to the top surface of CVD overgrown substrate under an optical microscope (Fig. 1e). The lateral dimensions of the frame were ~10% less than that of the substrate with a thickness in the range of 150–300 μm. The frame was temporarily attached to the top overgrown surface of the substrate by surface tension and van der Waals forces of the respective diamond materials. The assembly composed of diamond frame and overgrown substrate was then placed again in a MPCVD reactor for fusion growth under same conditions as shown in Fig. 1c, resulting in selective growth of a new SCD layer through the apertures of the frame, and the formation of a fusion layer of diamond material around the contact of the frame and overgrown substrate (Fig. 1f). The fused substrate was immersed in a boric acid solution and the graphite-like carbon layer was electrochemically etched away under constant voltage (~300 V) applied across two platinum electrodes (Fig. S1 in ESI†). In this way, the SCD membrane fused with diamond frame was separated and lifted off (Fig. 1g). The fusion was extremely strong and stable under mechanical force and it survived harsh chemical and acid treatments.

The membrane fused frame was flipped and the remaining ~1.7 μm damage layer caused by the ion implantation was removed using inductive coupled plasma reactive ion etching (ICP-RIE). An alternating sequence based mainly on two plasma types (Ar/Cl_2) and (O_2/Ar) was used for etching to achieve high surface quality.[28,29] Finally, the surface went through a very mild O_2 plasma to etch a few nanometres of diamond, preserving the as grown surface.[30] RIE was conducted until the desired thickness of SCD membrane windows was achieved (Fig. 1h). Membrane thicknesses were controlled by the RIE thinning rate, while a constant etch rate was confirmed throughout the process with white light interferometry measurement and SEM (see thickness measurement section in ESI†). Also, it is important to note that the thickness profile of the membrane windows is not affected by RIE within the apertures of diamond frame[9] (Fig. 1i), because our technique requires the removal of a relatively small thickness of material. Furthermore, an etching step through the diamond frame is not strictly necessary which may be attractive in some cases. A diamond cleaning process consisting of acid boiling in a mixture of concentrated sulphuric (H_2SO_4) and sodium nitrate ($NaNO_3$), at high temperature for ~15 minutes, was performed after every step of the process to remove any remaining graphite residue. This was followed by washing in acetone, methanol and isopropanol to remove surface contamination. Fig. 1j shows the cartoon of final SCDMW fabricated from this method. The diamond frame fused to the SCD membrane provided another advantage in preventing cracks and bowing during lift-off of the membrane and made possible fabrication of millimetre size large membranes. Handling of the SCD membranes was also manageable, allowing for flipping, transferring and for further processing.

3. Results

Fig. 2 shows the optical, scanning electron microscope (SEM), and atomic force microscope (AFM) micrographs of the SCDMW. Three batches consisting of 10 samples in total were fabricated to demonstrate the scalable and reproducible nature of fabrication process. Fig. 2(a–c) shows a top down view of the produced arrays of membrane windows. Type Ib ($4 \times 4 \times 0.5$ mm) original HPHT SCD substrate was used to fabricate 4×4 mm large membrane (Fig. 2a) and Type IIa ($3 \times 3 \times 0.3$ mm) CVD pristine substrate was diced into 1.5×1.5 mm

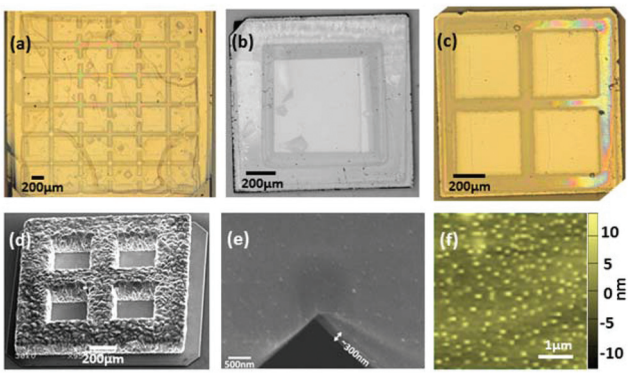

Fig. 2 (a) Optical micrograph of a large size 4 × 4 mm SCD membrane consisting of 6 × 6 arrays of membrane windows each with a size 400 × 400 μm connected *via* thin membrane micro-channels. Each membrane window can have multiple devices which can be linked *via* waveguides in these micro-channels. (b) Optical micrograph of 1.5 × 1.5 mm SCD membrane containing one large membrane window of size 800 × 800 μm within SCD frame. (c) Optical micrograph of 1.5 × 1.5 mm SCD membrane having 2 × 2 arrays of membrane windows of size 400 × 400 μm in a diamond frame. (d) SEM image after lift-off showing membrane and frame thickness. (e) SEM image of thin membrane window cross section showing thickness of ~300 nm and surface quality. (f) AFM scan (5×5 μm^2) of thin membrane window with root mean square (RMS) surface roughness of ~3 nm.

sizes, using laser micromachining to produce membranes of 1.5 × 1.5 mm for different experiments (Fig. 2b and c). Features like pyramids or pits in the membrane windows are observed for some samples, which are transferred from original substrates during CVD overgrowth step. Membrane surface quality can be improved by substrate preparation methods or selection of smooth and dislocation free substrate.[24] Fig. 2(d and e) shows SEM micrographs of the frame side view comprised 2 × 2 arrays of membrane windows after lift-off and the cross sectional view confirming the final SCDMW's thickness of ~300 nm after thinning respectively. AFM scan (5 × 5 μm^2) reveals a surface roughness of ~3 nm (Fig. 2f).

3.1. Raman measurements

The membrane windows were investigated at each processing stage with Raman spectroscopy using 532 nm laser to measure the diamond quality during fabrication (Fig. 3). In particular, the intensity and shape of the Raman spectrum at 1333 cm^{-1} (characteristic of sp^3 bonded carbon, single crystal diamond) was recorded. The Raman signature from as received bulk SCD is observed at 1333 cm^{-1} and has a full width half maximum (FWHM) of 2.3 cm^{-1} as shown in inset. The diamond peak at 1333 cm^{-1} is no longer apparent after ion implantation due to the damage created (although other peaks emerge). After annealing, the diamond lattice regains its crystallinity and the diamond peak re-emerges but with a larger FWHM at 1333 cm^{-1}. In addition, peaks at 1550 cm^{-1} (which is indicative of graphitic, damaged sp^2 carbon) and 2060 cm^{-1} can be observed. A stronger diamond peak signal and lower damage profile can be observed after the high quality CVD overgrowth step. The final step of RIE etching removes the remaining damage and as-grown diamond is revealed. At the end of processing we only observe diamond peak at 1333 cm^{-1} collected from thin SCDMW with comparable characteristics of as received SCD substrate. The FWHM of ~300 nm thin SCDMW is 2.1 cm^{-1} as shown inset which is comparable to the FWHM of the Raman line from the as received bulk substrate.

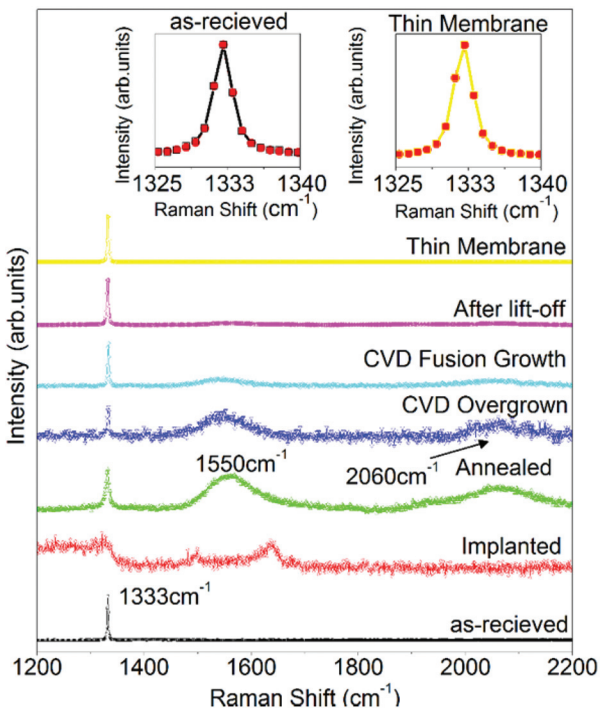

Fig. 3 Normalized Raman spectra after each stage of the fabrication process. The insets show the diamond-peak with a FWHM of 2.1 cm^{-1} and 2.3 cm^{-1} for a ~300 nm thin SCDMW and as-received bulk SCD substrate respectively.

3.2. Photo-luminescence (PL) measurements

To further examine the diamond quality, and suitability for hosting bright colour centers, we investigated the SCDMW with a single-photon sensitive confocal microscope (Fig. 4). A confocal scan of the membrane window (Fig. 4a) shows clearly resolvable optically active defects with a density of ~5 μm^{-2}. Photoluminescence (PL) spectra confirm that the centers are NVs showing signatures of NV^0 and NV^- at 575 nm and 637 nm respectively. The peak at 572 nm is the diamond Raman line (Fig. 4b). The studied optical centers showed good photostability and high count rates of ~200 kcounts per s (PL setup configuration provided in ESI†). Photon-antibunching measurements, performed with two avalanche photodetectors in Hanbury–Brown–Twiss arrangement, confirm that the investigated defects (highlighted as (1), (2) in Fig. 4a) are single photon emitters. A dip in the autocorrelation function to $g^2(0)$ = 0.3, after the background fluorescence is subtracted, indicates that most of the fluorescence arising from each spot highlighted in Fig. 4a can be attributed to individual colour

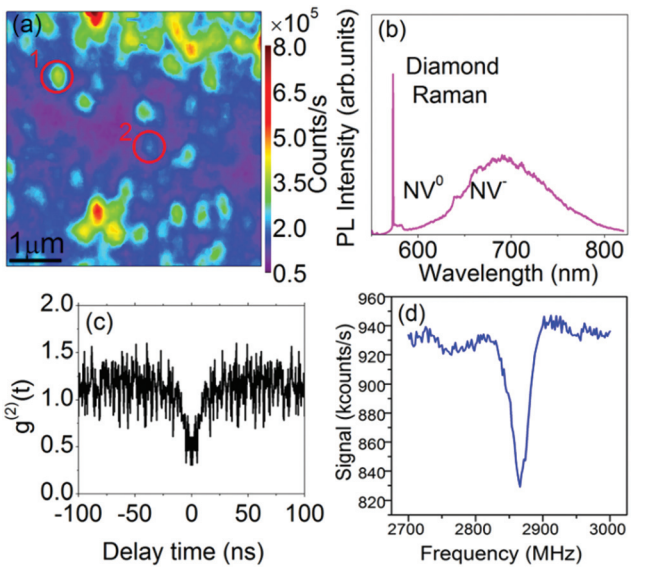

Fig. 4 (a) Confocal microscopy raster scan (5 × 5 μm^2) showing with two individual NVs identified. (b) PL of NV signature obtained from a ~300 nm SCDMW sample. (c) Normalized $g^{(2)}(t)$ recorded from single NV center shows a dip of $g^{(2)}(t)$ = 0.3 corresponds to a single photon emitter. (d) Optically detected magnetic resonance (ODMR) spectrum taken from single NV center without an external magnetic field.

centers (Fig. 4c). We observe optically detected magnetic resonance (ODMR) from a single NV center (marked in Fig. 4a) without external magnetic field as shown in Fig. 4d. There is no peak splitting in the ODMR signal, which suggests that there is low strain in the membrane.

3.3. Mechanical resonator measurements

In Fig. 5 we show laser Doppler vibrometer measurements of the drumhead mechanical resonator which is composed of a fully clamped and freely suspended SCD membrane. We used a ~1 μm thick SCD membrane window supported by ~150 μm thick PCD frame. The membrane was clamped in a square geometry of side length (L = 400 μm) as shown in Fig. 2(c). We observe higher order resonant modes at frequencies measured approximately 2 and 3 times (f_{12} and f_{22} respectively) the fundamental frequency (f_{11} ~ 247 kHz) by mechanically driving the membrane with piezoelectric actuation and monitoring the position response of the membrane optically. These peaks (f_{12} and f_{22}) correspond to the second and third order measured modes (Fig. 5b). In this experiment, the resonance frequency response of thin SCDMW was measured in air with laser Doppler vibrometery at room temperature. This is in good agreement with the expected values of 200 kHz (f_{11}), 360 kHz ($f_{21} \sim 1.8f_{11}$) and 578 kHz ($f_{22} \sim 2.9f_{11}$) predicted for a square membrane clamped on all sides using Coventor simulations. The simulation was performed for a fully clamped diamond membrane resonator model given thickness = 1 μm, surface area = 400 × 400 μm and material density = 3500 kg m^{-3}. A mechanical quality factor (Q) of ~400 is achieved in air at a measured fundamental frequency (f_{11}) of 247 kHz which is twice that of fully clamped single layer graphene resonators[31] and also comparable to the Q of 230 for short free standing diamond cantilevers of frequency 6.7 MHz measured in air.[10] The estimated resonant mode shapes at fundamental frequency (f_{11} ~ 200 kHz) and third harmonic (f_{22} ~ 578 kHz) is shown respectively (Fig. 5a and c). We observe comparable resonant mode shapes in the membrane at the measured frequencies. The resonant mode shape measured at third harmonic (f_{22} ~ 740 kHz) is shown in Fig. 5(d).

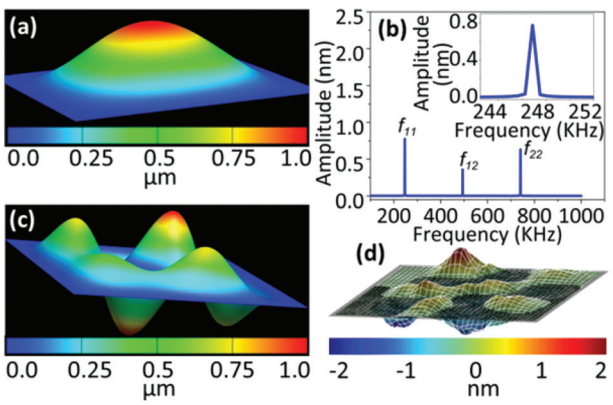

Fig. 5 SCD mechanical resonator (a) simulation of resonance of 1 μm thick fully clamped square SCD membrane window at estimated fundamental frequency 200 kHz. (b) Spectrum of all measured fundamental (f_{11}) and higher modes (f_{12} and f_{12}) for the SCDMW. The inset shows measured fundamental frequency of membrane with Q ~400. (c) The simulation of resonant mode shapes at estimated third harmonic 578 kHz in a diamond membrane. (d) Measured resonant mode shape of vibrations in the SCDMW observed at experimental third harmonic 740 kHz in air using laser Doppler vibrometery at room temperature.

4. Conclusion

In conclusion, we have presented a scalable method to fabricate ultra-thin, large area, high-quality SCDMW with optically-active colour centres. The method is used for successful fabrication of robust, large size, ultra-thin membranes fused to a thick diamond frame that enables easy handling of the membrane, allowing flipping, transferring and further processing. The Raman signature obtained from SCDMW shows high crystallinity and low strain. The SCDMW also hosts NV^- centers with single photon emission. The fully clamped and freely suspended thin SCDMW displays drum head resonances with a Q of ~400 in air. The scalable production of high quality SCDMW opens great prospects as a platform for on-chip devices for integrated photonics, quantum information processing and sensing devices.

Acknowledgements

This work was funded under the Australian Research Council (ARC) Linkage project (LP100100524) with industry partners Hewlett-Packard Laboratories and ARC Discovery Project (DP 1096288). S.T-H. is supported by an ARC Australian Research Fellowship (DP1096288). L.P.M is supported by the DAAD P.R.I.M.E. fellowship. This work was performed in part at the Melbourne Centre for Nanofabrication (MCN) in the Victorian Node of the Australian National Fabrication Facility (ANFF). The authors would like to thank Duc Huynh for assistance with Coventor simulations.

References

1 R. S. Balmer, J. R. Brandon, S. L. Clewes, H. K. Dhillon, J. M. Dodson, I. Friel, P. N. Inglis, T. D. Madgwick, M. L. Markham, T. P. Mollart, N. Perkins, G. A. Scarsbrook, D. J. Twitchen, A. J. Whitehead, J. J. Wilman and S. M. Woollard, *J. Phys.: Condens. Matter*, 2009, **21**, 364221.
2 A. M. Zaitsev, *Optical Properties of a Diamond*, Springer, Berlin, 2001.
3 I. Aharonovich, A. D. Greentree and S. Prawer, *Nat. Photonics*, 2011, **5**, 397–405.
4 A. Faraon, P. E. Barclay, C. Santori, K. M. C. Fu and R. G. Beausoleil, *Nat. Photonics*, 2011, **5**, 301.
5 S. Tomljenovic-Hanic, M. J. Steel, C. Martijn de Sterke and J. Salzman, *Opt. Express*, 2006, **14**, 3556.
6 S. Gsell, T. Bauer, J. Goldfuß, M. Schreck and B. Stritzker, *Appl. Phys. Lett.*, 2004, **84**, 4541.

7 J. Riedrich-Moller, L. Kipfstuhl, C. Hepp, E. Neu, C. Pauly, F. Mucklich, A. Baur, M. Wandt, S. Wolff, M. Fischer, S. Gsell, M. Schreck and C. Becher, *Nat. Nanotechnol.*, 2012, **7**, 69.
8 P. Maletinsky, S. Hong, M. S. Grinolds, B. Hausmann, M. D. Lukin, R. L. Walsworth, M. Loncar and A. Yacoby, *Nat. Nanotechnol.*, 2012, **7**, 320–324.
9 M. Pomorski, B. Caylar and P. Bergonzo, *Appl. Phys. Lett.*, 2013, **103**, 112106.
10 J. Teissier, A. Barfuss, P. Appel, E. Neu and P. Maletinsky, *Phys. Rev. Lett.*, 2014, **113**, 020503.
11 P. Ovartchaiyapong, L. M. A. Pascal, B. A. Myers, P. Lauria and A. C. B. Jayich, *Appl. Phys. Lett.*, 2012, **101**, 163505.
12 Y. Tao and C. Degen, *Adv. Mater.*, 2013, **25**, 3962.
13 B. J. M. Hausmann, B. Shields, Q. M. Quan, P. Maletinsky, M. McCutcheon, J. T. Choy, T. M. Babinec, A. Kubanek, A. Yacoby, M. D. Lukin and M. Loncar, *Nano Lett.*, 2012, **12**, 1578.
14 A. Faraon, C. Santori, Z. H. Huang, K.-M. C. Fu, V. M. Acosta, D. Fattal and R. G. Beausoleil, *New J. Phys.*, 2013, **15**, 025010.
15 P. Latawiec, V. Venkataraman, M. J. Burek, B. J. M. Hausmann, I. Bulu and M. Lončar, *Optica*, 2015, **2**, 924–928.
16 B. J. M. Hausmann, I. Bulu, V. Venkataraman, P. Deotare and M. Loncar, *Nat. Photonics*, 2014, **8**, 369.
17 J. S. Hodges, L. Li, M. Lu, E. H. Chen, M. E. Trusheim, S. Allegri, X. Yao, O. Gaathon, H. Bakhru and D. Englund, *New J. Phys.*, 2012, **14**, 093004.
18 O. Gaathon, J. S. Hodges, E. H. Chen, L. Li, S. Bakhru, H. Bakhru, D. Englund and R. M. Osgood Jr., *Opt. Mater.*, 2013, **35**, 361.
19 B. A. Fairchild, P. Olivero, S. Rubanov, A. D. Greentree, F. WaIdermann, R. A. Taylor, I. Walmsley, J. M. Smith, S. Huntington, B. C. Gibson, D. N. Jamieson and S. Prawer, *Adv. Mater.*, 2008, **20**, 4793.
20 A. Magyar, J. C. Lee, A. M. Limarga, I. Aharonovich, F. Rol, D. R. Clarke, M. B. Huang and E. L. Hu, *Appl. Phys. Lett.*, 2011, **99**, 081913.
21 J. C. Lee, A. P. Magyar, D. O. Bracher, I. Aharonovich and E. L. Hu, *Diamond Relat. Mater.*, 2013, **33**, 45.
22 I. Aharonovich, J. C. Lee, A. P. Magyar, B. B. Buckley, C. G. Yale, D. D. Awschalom and E. L. Hu, *Adv. Mater.*, 2012, **24**, OP54.
23 J. C. Lee, I. Aharonovich, A. P. Magyar, F. Rol and E. L. Hu, *Opt. Express*, 2012, **20**, 8891.
24 I. Friel, S. L. Clewes, H. K. Dhillon, N. Perkins, D. J. Twitchen and G. A. Scarsbrook, *Diamond Relat. Mater.*, 2008, **18**, 808–815.
25 J. F. Ziegler, *Nucl. Instrum. Methods Phys. Res., Sect. B*, 2004, **219–220**, 1027.
26 N. R. Parikh, J. D. Hunn, E. McGucken, M. L. Swanson, C. W. White, R. A. Rudder, D. P. Malta, J. B. Posthill and R. J. Markunas, *Appl. Phys. Lett.*, 1992, **61**, 3124.
27 C. Uzan-Saguy, C. Cytermann, R. Brener, V. Richter, M. Shaanan and R. Kalish, *Appl. Phys. Lett.*, 1995, **67**, 1194.
28 C. L. Lee, E. Gu, M. D. Dawson, I. Friel and G. A. Scarsbrook, *Diamond Relat. Mater.*, 2008, **17**, 1292.
29 C. L. Lee, E. Gu and M. D. Dawson, *Diamond Relat. Mater.*, 2007, **16**, 944.
30 F. Fávaro de Oliveira, S. A. Momenzadeh, Y. Wang, M. Konuma, M. Markham, A. M. Edmonds, A. Denisenko and J. Wrachtrup, 2015, arXiv preprint, arXiv:1507.00890.
31 A. M. Zande, R. A. Barton, J. S. Alden, C. S. Ruiz-Vargas, W. S. Whitney, P. H. Pham, J. Park, J. M. Parpia, H. G. Craighead and P. L. McEuen, *Nano Lett.*, 2010, **10**, 4869–4873.